Pygmy Resonances in Tin Isotopes

D. Tarpanov[1], Ch. Stoyanov[1], Nguyen Van Giai[2], and V. V. Voronov[3]

[1] Institute of Nuclear Research and Nuclear Energy, Bulgarian Academy of Sciences, 1784 Sofia, Bulgaria
[2] Institut de Physique Nucléaire, Université Paris-Sud, F-91406 Orsay Cedex, France
[3] Bogoliubov Laboratory of Theoretical Physics, Joint Institute for Nuclear Research, 141980 Dubna, Moscow Region, Russia

Abstract. A nuclear structure model based on finite rank approximation of Skyrme interaction is applied to calculate the distribution of dipole strength in tin isotopes. The model is based on Random Phase Approximation and includes pairing correlations. The results obtained using three types of parameterizations of the Skyrme forces (SLy4, SkM* and SIII) are compared. The low-lying part of dipole excitations reveals the existence of group of slightly collective states and the corresponding E1 transition strength increases with the enlargement of neutron excess. The group is associated with Pygmy resonance.

1 Introduction

In a recent experiment done at GSI, Darmstadt [1], the distribution of electric dipole strength in the unstable nuclei ^{130,132}Sn was measured. Together with some theoretical results [2–6], received within different theoretical approaches, it gives a hint for the existence of a low-lying dipole mode commonly referred as 'pygmy' dipole resonance (PDR). These excited states are known to be slightly collective – exhaust a few per cent of energy weighted sum rule (EWSR), and the collectivity increases with enlargement of the neutron excess. The tin isotopic chain includes 18 even-even nuclei in the domain between the neutron magical numbers 50 and 82 and it is quite suitable to study the dependence of the PDR on neutron excess. We have calculated the distribution of $E1$-strength along the chain ^{100}Sn–^{132}Sn. The structure of the excited states was calculated by means of 'quasi-particle random phase approximation' (QRPA). The residual particle-hole interaction is Skyrme type interaction. A method, known as finite rank approximation for RPA calculations with Skyrme interaction, is used [7–9]. The approximation is based on Landau-Migdal representation of Skyrme interaction [10]. The method proves as useful in large configurational space, where the problem with the diagonalization of the model Hamiltonian is avoided. The results of several applications about the structure of excited states in various nuclei are published [8, 9].

The Landau-Migdal representation of Skyrme interaction reads:

$$V_{ph} = N_0^{-1} \sum [F_l + G_l \sigma_1.\sigma_2 + (F'_l + G'_l \sigma_1.\sigma_2)\tau_1\tau_2] \times \delta(r_1 - r_2) \qquad (1)$$

Here σ and τ are the spin and the isospin operators. The representation (1) ensures self-consistence between mean field and $p - h$ residual interaction.

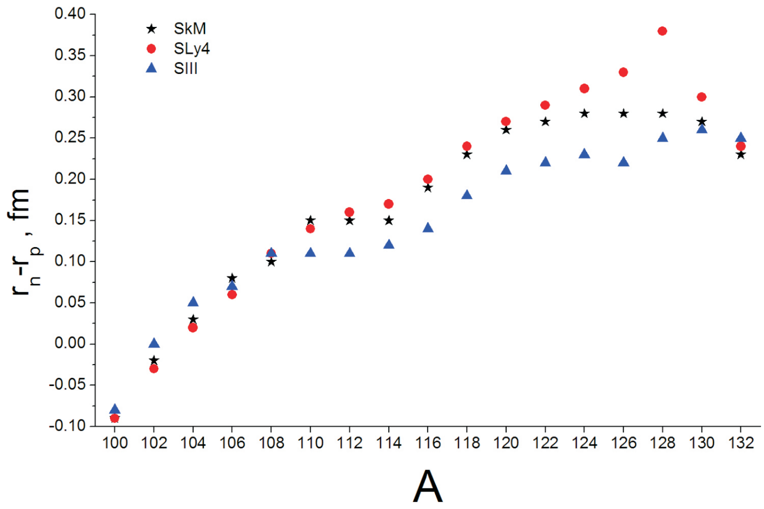

Figure **1.** The value of $r_n - r_p$, calculated with SkM*, SIII and SLy4 parameterization.

2 Results

In this work we use three types of parameterization of the Skyrme force. These are SkM*, SIII [11] and SLy4 [12]. Spherical symmetry is assumed for the Hartree–Fock (HF) ground state. The pairing constant is chosen in order the pairing gaps to have values close to $\Delta = 12.0A^{-1/2}$.

Of great importance for us is how well we reproduce the ground state properties of the stable nuclei, we pay a special interest on the nucleon radii. On Figure 1 the dependence of the difference between neutron and proton radii on the mass number is shown. The difference becomes larger when the number of the neutrons is increased. The calculated charge radii are in reasonable agreement with the known experimental data [13, 14]. The radii decrease about 10% around the double magic ^{132}Sn. It is because the pairing gap disappears for this nucleus. The distribution of $E1-$strength for ^{130}Sn is plotted on Figure 2. This distribution depends on the choice of the Skyrme force. For example, the centroid of the giant dipole resonance (GDR) is at 14.20 MeV for SkM*, 16.30 MeV for SLy4 and 14.85 MeV for SIII. It reflects on the behavior of the low-lying tail of the distribution. This is shown on Figure 3 for three different tin isotopes – ^{100,122,130}Sn, the strength of the corresponding QRPA states is smeared by Lorentzian with a scale parameter of 0.5 MeV. It is seen that for all three parameterizations the $E1-$strength below 10MeV enlarges when the neutron number is increased. This effect is shown in details on Table 1, where the $E1-$strength below 10.5 MeV for tin isotopic chain is shown. It is seen from Table 1 that when the mass number increases, greater strength is shifted downwards. The SkM* predicts quite large $E1-$strength below 10.5 MeV than the experimental one, [1], while SLy4 underestimates this value. $E1-$strength predicted by SIII for ^{100}Sn is larger in comparison of those of SkM* and SLy4.

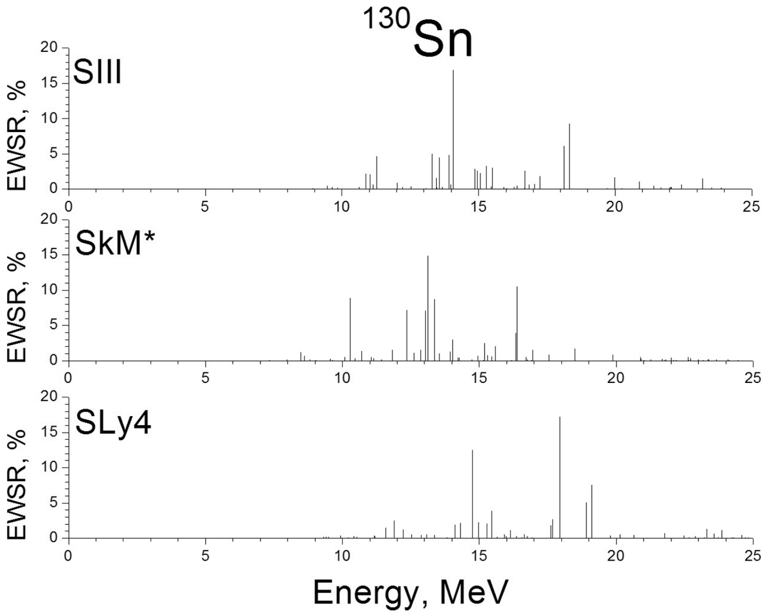

Figure **2.** The distribution of the E1 strength in ^{130}Sn, calculated with three different Skyrme parameterizations– SIII, SkM* and SLy4.

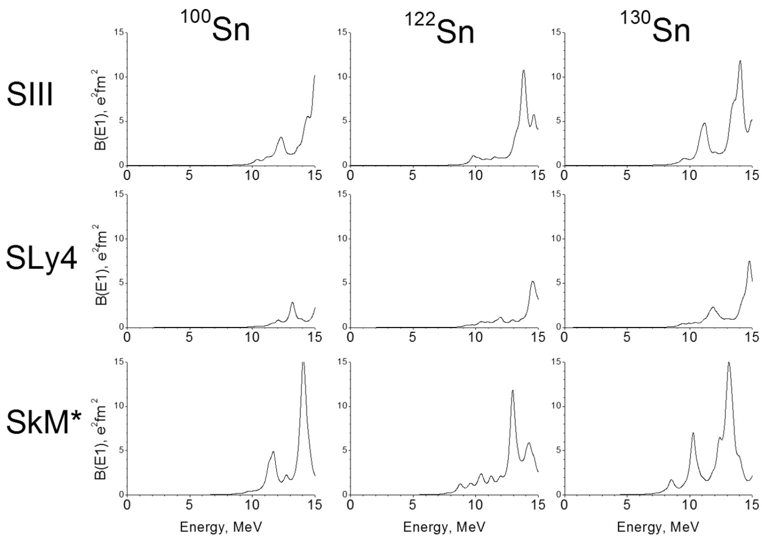

Figure **3.** The distribution of B(E1) up to 15 MeV for ^{100,122,130}Sn, calculated with SIII, SkM* and SLy4 Skyrme parameterization. The B(E1) values are smeared by Lorentz distribution with scale parameter of 0.5 MeV.

Table **1.** Summed $B(E1)$ values and their contribution in EWSR in the domain of excitation energy 0–10.5 MeV. Calculation is done within SkM*, SLy4 and SIII parameterization.

Nuclei	SkM*		SLy4		SIII	
	$B(E1)$, $e^2\text{fm}^2$	EWSR, %	$B(E1)$, $e^2\text{fm}^2$	EWSR, %	$B(E1)$, $e^2\text{fm}^2$	EWSR, %
^{100}Sn	0.93	0.62	0.21	0.21	1.44	0.96
^{102}Sn	1.17	0.76	0.24	0.24	0.19	0.13
^{104}Sn	1.00	0.66	0.01	0.06	0.23	0.15
^{106}Sn	0.92	0.62	0.31	0.31	0.26	0.17
^{108}Sn	0.92	0.64	0.32	0.32	0.27	0.17
^{110}Sn	1.03	0.72	0.43	0.43	0.25	0.16
^{112}Sn	1.02	0.72	0.24	0.24	0.24	0.16
^{114}Sn	1.00	0.70	0.31	0.31	0.40	0.27
^{116}Sn	1.50	1.01	0.62	0.62	0.30	0.20
^{118}Sn	2.42	1.59	0.78	0.78	1.17	0.77
^{120}Sn	6.25	4.19	1.87	1.87	3.28	2.13
^{122}Sn	10.6	7.33	2.24	2.24	3.65	2.37
^{124}Sn	11.0	7.59	2.41	2.41	3.62	2.33
^{126}Sn	12.7	8.88	2.56	2.56	3.29	2.19
^{128}Sn	16.5	12.0	2.22	2.22	2.47	1.60
^{130}Sn	17.8	13.1	2.44	2.44	1.84	1.20
^{132}Sn	13.8	10.2	2.09	2.09	1.42	0.91

It is because of the proton two-quasiparticle state $[2d_{3/2}2p_{1/2}]_\pi$. This fragment exhausts 75.62% of the state at 10.38 MeV. For SkM* and SLy4 the strength of this component is fragmented over several excited states.

The structure of a few excited states is presented in Table 2. the state at 13.13 MeV for SkM* as well as that at 14.08 MeV for SIII belongs to GDR. There are non-collective as well as slightly collective states at the low-energy tail of the $E1$-strength distribution. In ^{130}Sn the first few RPA states are dominated by one two-quasiparticle component. For the first state it is about 98%. This results (for the low-lying) states are in agreement with the results of Tzoneva [2, 3]. On the other hand Sarchi *et al.* [6] and Vretenar *et al.* [4] show that the low-lying excitations should be collective, we obtain such states at higher energies.

3 Conclusions

The properties of the electric dipole excitation in tin isotopic chain are calculated within $QRPA$. Three types of Skyrme interaction are used in the calculations. They reveal different distribution of $E1$ strength. It is shown that the contribution of $E1$ transition probability in the low-lying tail of the distribution enlarges with the increasing of neutron number. To obtain precise comparison with the available experimental data it is necessary to go beyond $QRPA$ and to take into account the phonon coupling.

Table **2.** Structure of the states for ^{130}Sn, obtained within the RPA framework, for SkM* and SIII parameterizations. Only the dominant neutron and proton components are shown. The index 'ν' denotes neutron configurations and 'π' – proton.

	SkM*		
Energy [MeV]	configuration	$B(E1)\uparrow$ [e^2fm^2]	EWSR [%]
8.62	$90.43\%[3p_{1/2}2d_{3/2}]_\nu + 1.07\%[2f_{7/2}2d_{5/2}]_\nu + 1.68\%[2d_{5/2}2p_{3/2}]_\pi$	0.43	0.675
10.27	$32.60\%[1h_{9/2}1g_{7/2}]_\nu + 19.10\%[1g_{7/2}1f_{5/2}]_\pi + 17.04\%[1i_{13/2}1h_{11/2}]_\nu$ $9.48\%[1h_{11/2}1g_{9/2}]_\nu + 8.72\%[3p_{3/2}2d_{5/2}]_\nu + 2.86\%[2d_{5/2}1f_{5/2}]_\pi$	4.78	8.85
13.13	$27.45\%[4p_{3/2}2d_{3/2}]_\nu + 24.17\%[4s_{1/2}2d_{3/2}]_\nu + 10.21\%[2d_{3/2}1f_{5/2}]_\pi$ $7.90\%[1h_{9/2}1g_{7/2}]_\nu + 4.85\%[1i_{13/2}1h_{11/2}]_\nu + 4.61\%[1g_{7/2}1f_{5/2}]_\nu$	6.25	14.83
	SIII		
Energy [MeV]	configuration	$B(E1)\uparrow$ [e^2fm^2]	EWSR [%]
9.46	$91.91\%[3p_{1/2}2d_{3/2}]_\nu + 6.84\%[3p_{3/2}3s_{1/2}]_\nu$ $2.64\%[1i_{13/2}1h_{11/2}]_\nu + 1.14\%[1h_{11/2}1g_{9/2}]_\pi$	0.28	0.48
11.26	$20.66\%[1i_{13/2}1h_{11/2}]_\nu + 17.43\%[1h_{9/2}1g_{7/2}]_\nu + 9.11\%[3p_{3/2}2d_{5/2}]_\nu$ $8.80\%[2d_{5/2}2p_{3/2}]_\pi + 8.71\%[1g_{7/2}1f_{5/2}]_\pi + 7.32\%[1h_{11/2}1g_{9/2}]_\nu$ $6.88\%[3s_{1/2}2p_{1/2}]_\pi + 6.08\%[2d_{3/2}2p_{1/2}]_\pi + 5.20\%[2f_{7/2}2d_{5/2}]_\nu$	2.27	4.62
14.08	$22.72\%[4p_{1/2}3s_{1/2}]_\nu + 11.10\%[2d_{3/2}1f_{5/2}]_\pi + 8.92\%[3f_{5/2}2d_{3/2}]_\nu$ $7.23\%[1g_{7/2}1f_{5/2}]_\pi + 6.07\%[1h_{11/2}1g_{9/2}]_\pi + 5.40\%[3s_{1/2}2p_{1/2}]_\nu$ $4.82\%[1h_{9/2}1g_{7/2}]_\nu + 3.86\%[1g_{7/2}1f_{7/2}]_\pi + 3.35\%[2d_{3/2}2p_{1/2}]_\nu$	6.65	16.90

Acknowledgments

This work is partly supported by Bulgarian Science Foundation (contr. Ph. 1311, VUF06/05, project CECOA).

References

1. P. Adrich *et al.*, *Phys. Rev. Lett.* **95**, 132501 (2005).
2. N. Tsoneva, H. Lenske and Ch. Stoyanov, *Nucl. Phys. A* **731**, 273 (2004).
3. N. Tsoneva, H. Lenske and Ch. Stoyanov, *Phys. Lett. B* **586**, 213 (2004).
4. D. Vretenar, N. Paar, P. Ring, G. Lalazissis, *Nucl. Phys. A* **692**, 496 (2001).
5. N. Paar, T. Nikšić, D. Vretenar, P. Ring, *Phys. Lett. B* **606**, 288 (2005).
6. D. Sarchi, P. F. Bortignon, G. Colo, *Phys. Lett. B* **601**, 27 (2004).
7. Nguyen Van Giai, Ch. Stoyanov, V. V. Voronov, *Phys. Rev. C* **57**, 1204 (1998).
8. A. P. Severyukhin, Ch. Stoyanov, V. V. Voronov, Nguyen Van Giai, *Phys. Rev. C* **66**, 034304 (2002).
9. A. P. Severyukhin, V. V. Voronov, Ch. Stoyanov, Nguyen Van Giai, *Phys. of Atomic Nuclei* **66**, 1434 (2003).
10. Nguyen Van Giai, H. Sagawa, *Phys. Lett. B* **106**, 79 (1981).

11. E. Chabanat, P. Bonche, P. Haensel, J. Meyer, R. Schaeffer, *Nucl. Phys. A* **627**, 710 (1997).
12. E. Chabanat, P. Bonche, P. Haensel, J. Meyer, R. Schaeffer, *Nucl. Phys. A* **635**, 231 (1998); *Nucl. Phys. A* **(**643), 441 (1998).
13. E. Nadzakov *et al.*, *Atomic Data and Nuclear Data Tables*, 56(1) (1994).
14. F. Le Blanc *et al.*, *Phys. Rev. C* **72**, 034305 (2005).